

# Linear/Nonlinear Behavior in Unsteady Transonic Aerodynamics

Earl H. Dowell\*

*Princeton University, Princeton, New Jersey*

Samuel R. Bland†

*NASA Langley Research Center, Hampton, Virginia*  
and

Marc H. Williams‡

*Princeton University, Princeton, New Jersey*

The accurate calculation of the aerodynamic forces in unsteady transonic flow requires the solution of the nonlinear flow equations. The aeroelastician, on the other hand, seeks to treat his problems (flutter, for example) by means of linear equations whenever possible. He may do this, even when the underlying flow is nonlinear, if the perturbation forces are linear over some (perhaps small) range of unsteady amplitude of motion. This paper assesses the range of parameters over which linear behavior occurs. In particular, calculations are made for an NACA 64A006 and also an MBB-A3 airfoil oscillating in pitch over a range of amplitudes, frequencies, and Mach numbers. The primary aerodynamic method used is the well known LTRAN2 code of Ballhaus and Goorjian that provides a finite difference solution to the low frequency, small disturbance, two-dimensional potential flow equation. Comparisons are made with linear subsonic theory, local linearization theory, and, for steady flow, with the full potential equation code of Bauer, Garabedian, and Korn in both its conservative and nonconservative form.

## Nomenclature

$C_L, C_M$	= lift, moment coefficients
$C_{L\alpha}, C_{M\alpha}$	= lift, moment curve slopes
$C_p, \bar{C}_p$	= pressure coefficients
$c$	= airfoil chord
$K$	= $(\gamma + 1)M_\infty^2 \tau / \beta^3$
$k$	= $\omega c / U_\infty$ ; reduced frequency
$M$	= Mach number
$s$	= $(\beta^2 t U_\infty / c) / M_\infty^2$
$t$	= time
$x, y$	= spatial coordinates in freestream and vertical directions
$x_s$	= shock location
$\Delta x_s$	= shock displacement normalized by the airfoil chord
$\alpha_0, \alpha_1$	= mean angle of attack; dynamic angle of attack in degrees
$\beta$	= $(1 - M_\infty^2)^{1/2}$
$\gamma$	= ratio of specific heats
$\nu$	= $k M_\infty^2 / \beta^2$
$\phi$	= phase angle
$\tau$	= thickness ratio of airfoil
$\omega$	= frequency

## Subscripts

$\infty$	= freestream
$L$	= local; also lift
$M$	= moment
max	= maximum
0, 1	= mean, dynamic
TE	= trailing edge

## Superscripts

$c$	= shock first forms
$tc$	= shock reaches the trailing edge

## I. Introduction, Motivation, and General Background

THE aeroelastician uses linear dynamic system theory for most aeroelastic analyses. The motivation for doing so is clear. Extensive experience, understanding, and effective computational/experimental procedures have been developed for linear systems. By contrast, although nonlinear methods of analysis and experimentation are available, the results are far more expensive to obtain and also more difficult to interpret. Hence linear models, where applicable, are very powerful, relatively simple, and extremely valuable. Thus, it is highly important to determine the domain of validity of any linear model.

Here our concern is with possible aerodynamic nonlinearities in transonic flow. Of course, aerodynamic nonlinearities may arise in other flow regimes; however, it is in transonic flow where they tend to be most important. Indeed, it is often observed that the transonic flow regime is inherently nonlinear in the governing field equations. However, at any Mach number for any airfoil, if the angle of attack is sufficiently small, the aerodynamic forces and shock motion will be linear in the angle of attack. Moreover, as the frequency of the angle of attack motion increases, the range of angle of attack over which linear behavior persists increases. It is our purpose here to study when linear or nonlinear behavior occurs using as our principal analytical method the low frequency, transonic small disturbance (LTRAN2) procedure of Ballhaus and Goorjian.<sup>1,2</sup> Any other present or future nonlinear aerodynamic method could (and should) be used for similar purposes.

Although LTRAN2 is our principal focus, results from other methods of analysis and experiment are available for comparison. In this respect it is of interest to display the results of Fig. 1, which show lift divided by angle of attack for an NACA 64A010 airfoil at  $M_\infty = 0.8$  for various reduced frequencies. The mean steady angle of attack is  $\alpha_0 = 0$  deg, and the dynamic angle of attack is  $\alpha_1 = 1.0$  deg. Results from several theories and one experiment<sup>3</sup> are shown. Except for flow separation, not accounted for by current inviscid transonic aerodynamic methods, Davis<sup>3</sup> observed no

Presented as Paper 81-0643 at the AIAA Dynamics Specialists Conference, Las Vegas, Nev., Atlanta, Ga., April 9-10, 1981; submitted April 27, 1981; revision received April 19, 1982. Copyright © American Institute of Aeronautics and Astronautics, Inc., 1981. All rights reserved.

\*Professor, Mechanical and Aerospace Engineering. Member AIAA.

†Aerospace Technologist, Unsteady Aerodynamics Branch. Member AIAA.

‡Research Staff, Mechanical and Aerospace Engineering; presently, Assistant Professor, Dept. of Aeronautics and Astronautics, Purdue University, West Lafayette, Ind. Member AIAA.

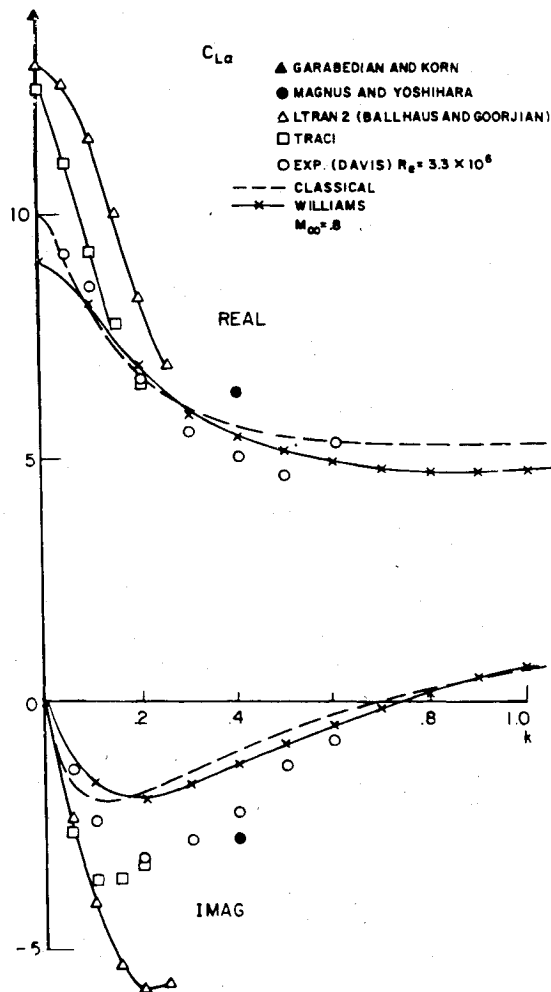


Fig. 1 Comparison of several theories with experiment. Pitch about quarter-chord lift.

significant nonlinearities in  $\alpha_l$  in his experiment. The various theoretical methods whose results are shown are:

1) Classical theory—i.e., the airfoil thickness is set to zero and the mean flow is uniform everywhere.

2) Williams' theory<sup>4,5</sup>—linear in  $\alpha_l$ ; theoretical or experimental data are used to locate the steady state shock and its strength which are determined by  $(\alpha_0)$  and the airfoil profile; the flow ahead and behind the shock is taken as uniform in the current version of the method, but the shock moves as  $\alpha_l$  varies.

3) LTRAN2<sup>1,2</sup>—nonlinear in (both  $\alpha_0$  and)  $\alpha_l$ ; transonic small disturbance theory; low frequency. See Yang<sup>6</sup> for these specific results.

4) TRACI—nominally the same as LTRAN2, but linear in  $\alpha_l$  with a less satisfactory treatment of the shock. See Yang<sup>6</sup> for these specific results.

5) Magnus<sup>7</sup>—solution of the complete, nonlinear, inviscid Euler equations; nonpotential.

Also shown is a steady flow result using the well known potential flow method of Bauer, Garabedian, and Korn.<sup>8</sup> The BGK result is obtained using a nonconservative finite difference algorithm. These results, although only for one Mach number and one airfoil, remind one that what constitutes a best theory depends upon the particular flow conditions, common deficiencies of all available theories, e.g., omission of viscosity, and the eye of the beholder. See Williams<sup>5</sup> for other comparisons of his method and LTRAN2 with Tijdeman's experiments.<sup>9</sup> It should be noted that comparisons of theory with experiment for *chordwise pressure distributions* show the clear superiority of Williams' theory and LTRAN2 over classical theory. See Williams<sup>5</sup> and the discussion below.

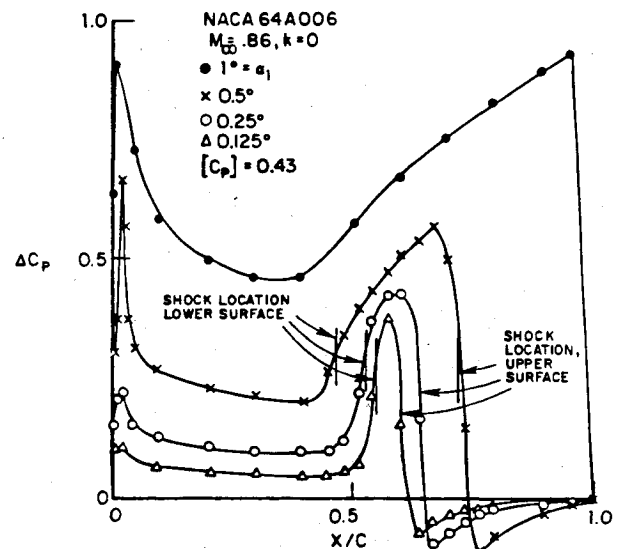


Fig. 2 Differential pressure distribution.

It will be helpful to discuss the shock and its motion which is sometimes a source of confusion. A consequence of any consistent linearization of unsteady transonic small disturbance aerodynamic theory in the *dynamic* angle of attack is that a concentrated force (sometimes called a shock doublet) will appear at the location of the steady state shock.<sup>4,5</sup> The strength of this force is equal to the steady state shock pressure jump and its width is proportional to the dynamic angle of attack. By contrast elsewhere on the airfoil chord (away from the shock doublet whose center is at the steady state shock location) the pressure magnitudes (in a *transonic* linear theory) are proportional to the dynamic angle of attack and become smaller in proportion as the dynamic angle of attack is smaller. Of course this latter behavior is also true in *classical* theory. The most important (although not the only) distinction between classical, linear theory and transonic, linear theory is the presence of the shock (and its motion) in the latter which creates the concentrated shock force doublet. LTRAN2 includes both the shock and its motion while classical aerodynamic theory includes neither. Some inconsistent transonic methods include the shock's presence, but not its motion.

The behavior described above is seen in a *nonlinear* dynamic theory as well, when the dynamic angle of attack becomes small. Consider Fig. 2 which was obtained using LTRAN2. It shows the chordwise differential (lower surface minus upper) pressure distribution for an NACA 64A006 airfoil at  $M_\infty = 0.86$  for several angles of attack. Here, for simplicity, the reduced frequency is set to zero so there is no distinction (numerically) between steady and dynamic angle of attack. As may be seen for small angles of attack, say  $\alpha = 0.125$  deg,  $0.25$  deg, the pressure distribution has a shock doublet centered at the mean (angle of attack) shock location,  $x_s/c = 0.584$ . The width of the shock doublet is indicated by the vertical lines, the forward one is at the lower surface shock location and the rearward one at the upper surface location. The shock doublet width is proportional to  $\alpha$  for the smaller  $\alpha$ ; however, as  $\alpha$  increases to  $1$  deg the lower surface shock disappears while the upper surface shock moves to the trailing edge and remains there. Also for the smaller  $\alpha$  the shock doublet magnitude is essentially equal to the pressure jump through the shock at  $\alpha = 0$  deg, i.e.,  $0.43$ . Away from the shock doublet, the pressures are proportional to  $\alpha$  for small  $\alpha$ . Finally, note a matter of practical importance. For small  $\alpha$  as the shock doublet width narrows, any finite difference scheme nonlinear in  $\alpha$  will have a resolution problem as  $\alpha \rightarrow 0$ . By contrast a method a priori linearized in  $\alpha$  avoids this difficulty as it computes the shock motion explicitly, e.g., see Williams<sup>4,5</sup> and Fung et al.<sup>10</sup> Also see the discussion of

Tijdeman<sup>11</sup> and Tijdeman and Seebass<sup>12</sup> for a critical assessment of theory and experiment.

We now turn to the five major issues which are listed below. These issues are first addressed for one airfoil, NACA 64A006, at one Mach number, 0.86, which is pitching in simple harmonic motion about its leading edge. Subsequently other Mach numbers are considered. For a more complete account of the present work, including a study of the MBB-A3 supercritical airfoil, see Ref. 13. The results for the supercritical airfoil are qualitatively similar to those for the NACA 64A006 and hence are omitted in the interest of brevity. The present calculations were carried out using a grid mesh of  $113 \times 97$ . Krupp rather than Sprieter transonic scaling was used, although a few calculations with the latter showed little difference.<sup>13</sup>

## II. NACA 64A006 Airfoil at $M_\infty = 0.86$ Pitching about its Leading Edge

The following principal issues were studied<sup>13</sup>: effect of dynamic angle of attack at various reduced frequencies on dynamic forces and shock motion; boundary for linear/nonlinear behavior; effect of reduced frequency and dynamic amplitude on aerodynamic transfer functions; effect of dynamic angle of attack on steady state forces and shock displacement; and effect of steady-state angle of attack on dynamic forces and shock motion.

### Effect of Dynamic Angle of Attack at Various Reduced Frequencies on Dynamic Forces and Shock Motion

It is desirable to assess at what dynamic amplitude nonlinear effects become important in order to determine the relative linear vs nonlinear behavior of lift, pitching moment, and shock motion. Note that the total lift (moment, shock motion) is characterized by  $C_L = C_{L_0} + C_{L_1}$ , where  $C_{L_0}$  is defined to be the lift due to  $\alpha_0$  and  $C_{L_1}$  that due to  $\alpha_1$  for a given  $\alpha_0$ . In classical linear theory (but not transonic linear theory)  $C_{L_1}$  is independent of  $\alpha_0$ .

In Figs. 3 and 4 lift, pitching moment, and shock displacement amplitudes are shown as a function of dynamic amplitude,  $\alpha_1$ , for reduced frequencies of  $k=0$ , and 0.2. Lift and moment coefficient have their usual definitions and the moment is about the midchord. The shock displacement is normalized by the airfoil chord. For  $k \neq 0$ , phases are also presented for lift and pitching moment. The shock motion phase was also computed; however, it tended to be less accurately determined.<sup>13</sup> Since it is not needed for our present purposes, it is not shown.

It is seen that lift tends to remain linear to higher dynamic amplitudes than moment which, in turn, tends to remain linear to higher amplitudes than shock motion. Moreover, the larger the reduced frequency, the greater the range of linear behavior. Phase information generally, although not universally, is a more sensitive indicator of departure from linearity than lift, moment, or shock amplitude information. In a strictly linear theory, of course, the phase is independent of the dynamic angle of attack.

It is noted that no measurable higher harmonic content was found in any of the numerical results. The results were virtually sinusoidal signals for lift, moment, and shock motion; hence, determination of magnitude and phase was readily done by any one of several conventional methods. The exception was shock motion phase which is difficult to determine accurately by any method because of the relatively coarse finite difference mesh resolution of the shock.

### Boundary for Linear/Nonlinear Behavior

It is highly desirable to provide a criterion by which the aeroelastician may assess when a linear dynamical theory may be used.

Figure 5 has been constructed from Fig. 3 and other similar results<sup>13</sup> by identifying the  $k, \alpha_1$  combinations for which the

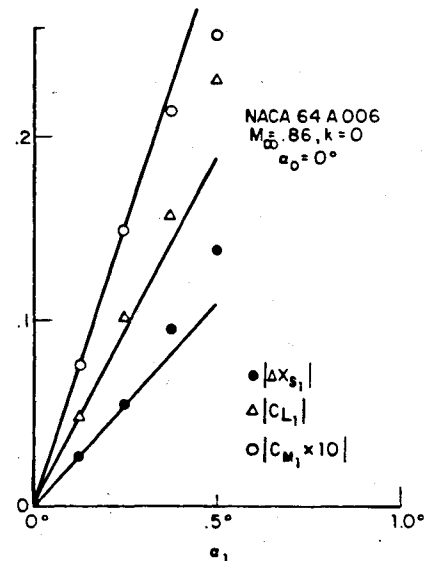


Fig. 3 Effect of dynamic angle of attack on dynamic forces and shock motions: amplitudes.

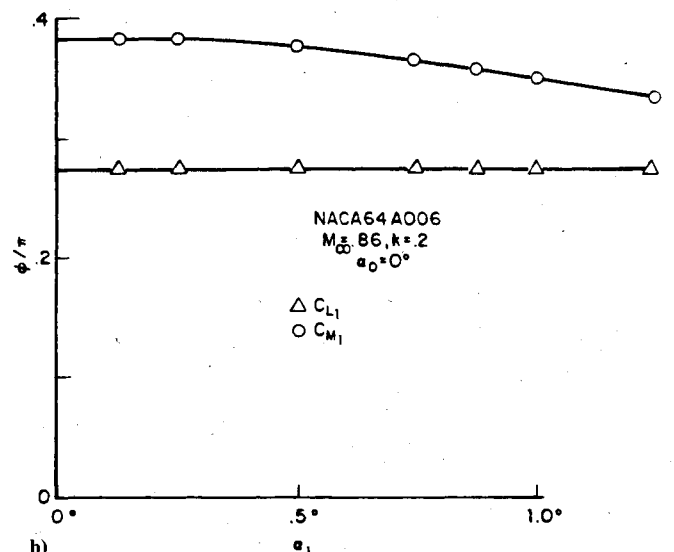
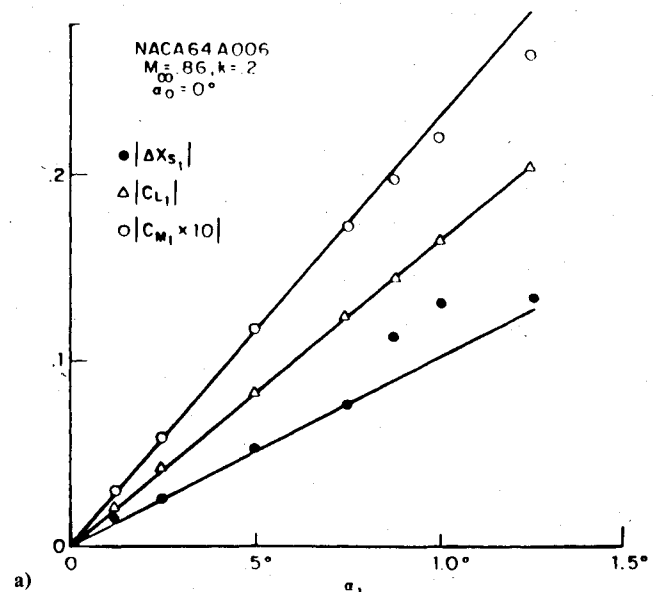


Fig. 4 Effect of dynamic angle of attack on dynamic forces and shock motions: a) amplitudes; b) phases.

pitching moment deviates by 5% in amplitude or phase from linearity. As expected at higher  $k$ , the pitching moment remains linear to larger  $\alpha_1$ .

Although Fig. 5 provides very useful information, it requires a *nonlinear dynamical* theory to construct it. A question arises: Is there a similar, but perhaps more conservative, criterion which may be used with a *linear dynamical* theory? The answer is provided by the shock motion. In Fig. 6 a similar boundary to that shown in Fig. 5 is constructed (again from the information provided by Figs. 3 and 4) based upon shock motion rather than pitching moment. It is observed in Figs. 3 and 4 that for shock displacement amplitudes of less than 5% the shock motion (as well as lift and pitching moment) behave in a linear fashion. Hence, a 5% shock motion boundary is shown in Fig. 6. Note that this boundary could be constructed from a *linear dynamical* theory. A second boundary (less conservative) based upon the first detectable deviation of shock motion from linearity is also shown. Finally, the boundary from Fig. 5 is shown for reference. These results are consistent with those of Ballhaus and Goorjian,<sup>2</sup> who also suggested that shock motions of less than 5% chord correspond to linear behavior.

Thus it is concluded that a simple criterion for departure from nonlinearity based upon shock motion may be used. It can be evaluated by a *linear dynamical* theory in principle (which enhances its practical utility), although the present results were obtained using a nonlinear, dynamical theory. Figures 5 and 6 describe a principal result of the present work.

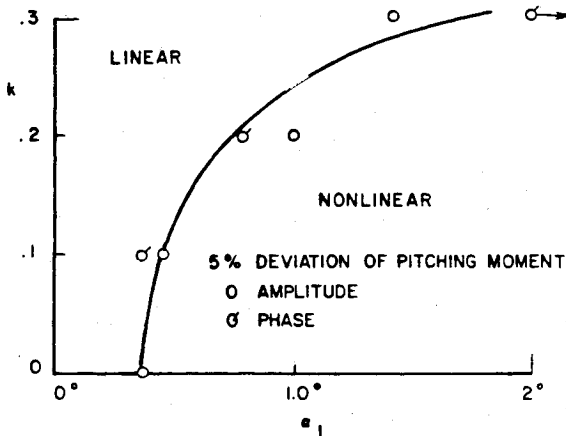


Fig. 5 Boundary for linear/nonlinear behavior in terms of reduced frequency and dynamic angle of attack.

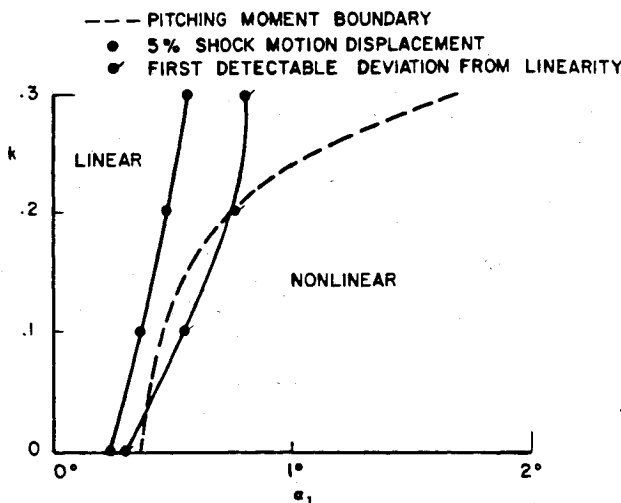


Fig. 6 Conservative boundary for linear/nonlinear behavior based upon shock motion amplitude.

A brief digression is in order to explain why the shock motion criterion is extremely useful to the aeroelastician. After the flutter mode is determined from a conventional flutter analysis using linearized, but transonic aerodynamics, one may compute the amplitude of the flutter motion which will correspond to a 5% shock motion using the *linear transonic* aerodynamic model employed in the flutter analysis. This will give the aeroelastician the limit on amplitude for which the linear, flutter calculation is valid. This is very useful information.

#### Effect of Reduced Frequency and Dynamic Amplitude on Aerodynamic Transfer Functions

We wish to determine when linear aerodynamic transfer functions are adequate and, when they are not, to provide information for characterizing nonlinear aerodynamic transfer (describing) functions. Accomplishing this purpose fully requires aeroelastic studies using the present (or similar) aerodynamic data. Here only the aerodynamic aspects are considered.

The aerodynamic transfer functions  $C_L/\alpha_1$ ,  $C_{M1}/\alpha_1$ ,  $\Delta x_{s1}/\alpha_1$  are plotted in Figs. 7-9 vs  $k$  for  $\alpha_1 = 0.25, 0.5$ , and  $1$  deg. As expected for  $k \rightarrow 0.3$ , the aerodynamic transfer functions are independent of  $\alpha_1$ , but for  $k \rightarrow 0$  they become discernible functions of  $\alpha_1$ . Only amplitudes are shown;

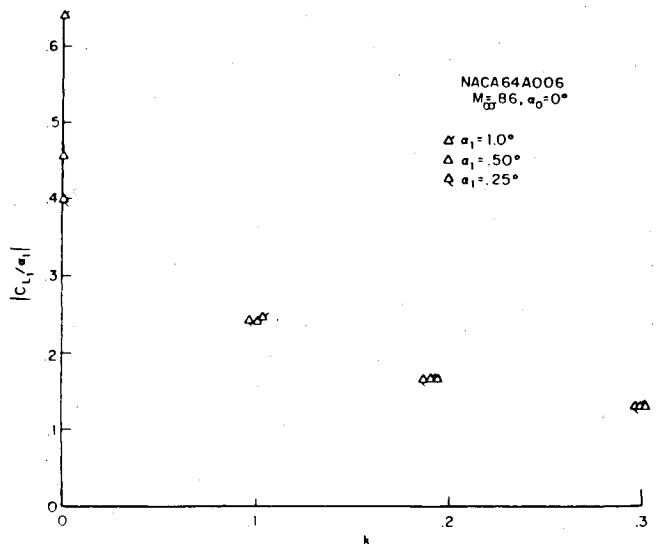


Fig. 7 Effect of reduced frequency and dynamic amplitude on lift transfer function: amplitudes.

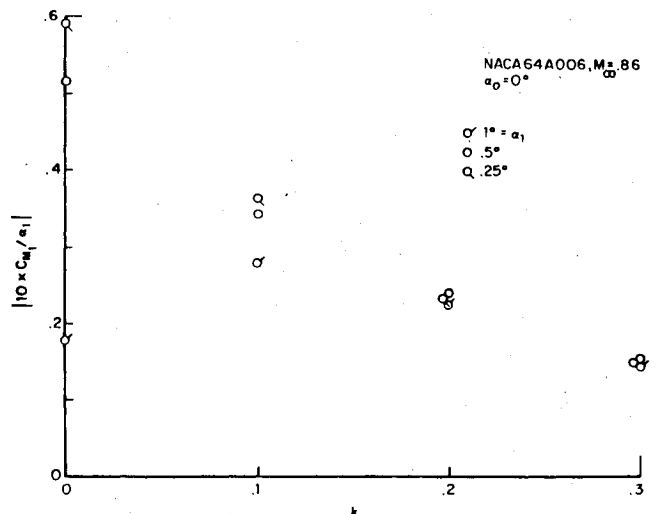


Fig. 8 Effect of reduced frequency and dynamic amplitude on moment transfer function: amplitudes.

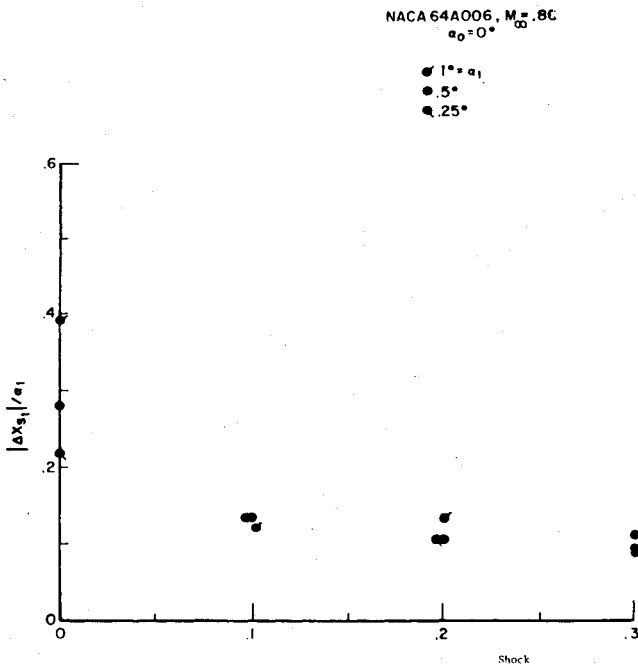


Fig. 9 Effect of reduced frequency and dynamic amplitude on shock transfer function: amplitudes.

phases of the transfer functions are omitted for the sake of brevity.<sup>13</sup>

For  $k \geq 0.2$ , linear aerodynamic transfer functions may be used with good accuracy. For  $k \rightarrow 0$  aerodynamic describing functions may be constructed and may be required in aeroelastic analyses.

#### Effect of Dynamic Angle of Attack on Mean, Steady-State Forces and Shock Displacement

Tentatively it is concluded that the effect of dynamic angle of attack on mean, steady-state forces and shock displacement is small. For more detailed discussion of the issue, see Ref. 13.

#### Effect of Steady State Angle of Attack on Dynamic Forces and Shock Motion

Next consider the effect of various steady flowfields on dynamic aerodynamic forces. From a dynamics point of view, changing steady-state angle of attack,  $\alpha_0$ , is in many ways analogous to changing the airfoil or flow Mach number. All of these give a new static equilibrium flow condition about which dynamic perturbations take place.

Figure 10 displays amplitude and phase of the dynamic lift, moment, and shock motions vs  $\alpha_0$  for one reduced frequency, 0.2, and one dynamic angle of attack,  $\alpha_1 = 0.5$ .  $\alpha_0 = 0.25 - 0.5$  is a rough boundary between modest and substantial effects. Clearly the effect of *mean* angle of attack,  $\alpha_0$ , on the dynamic aerodynamic forces can be substantial, comparable to the effect of airfoil profile or Mach number. This, of course, does *not* mean, necessarily, that there are nonlinear dynamic effects. It does suggest that the characterization of the steady flow about the airfoil is important in assessing its dynamic aerodynamic forces, be the latter linear or nonlinear in  $\alpha_1$ .

### III. Mach Number Trends

Here the effects of Mach number are studied systematically for the NACA 64A006 airfoil. We note that a similarity rule holds for low frequency, transonic flow which gives the following results for any family airfoils.

$$C_p = \frac{\tau}{\beta} \bar{C}_p(x/c; s; K, \nu, \alpha/\tau) \quad (1)$$

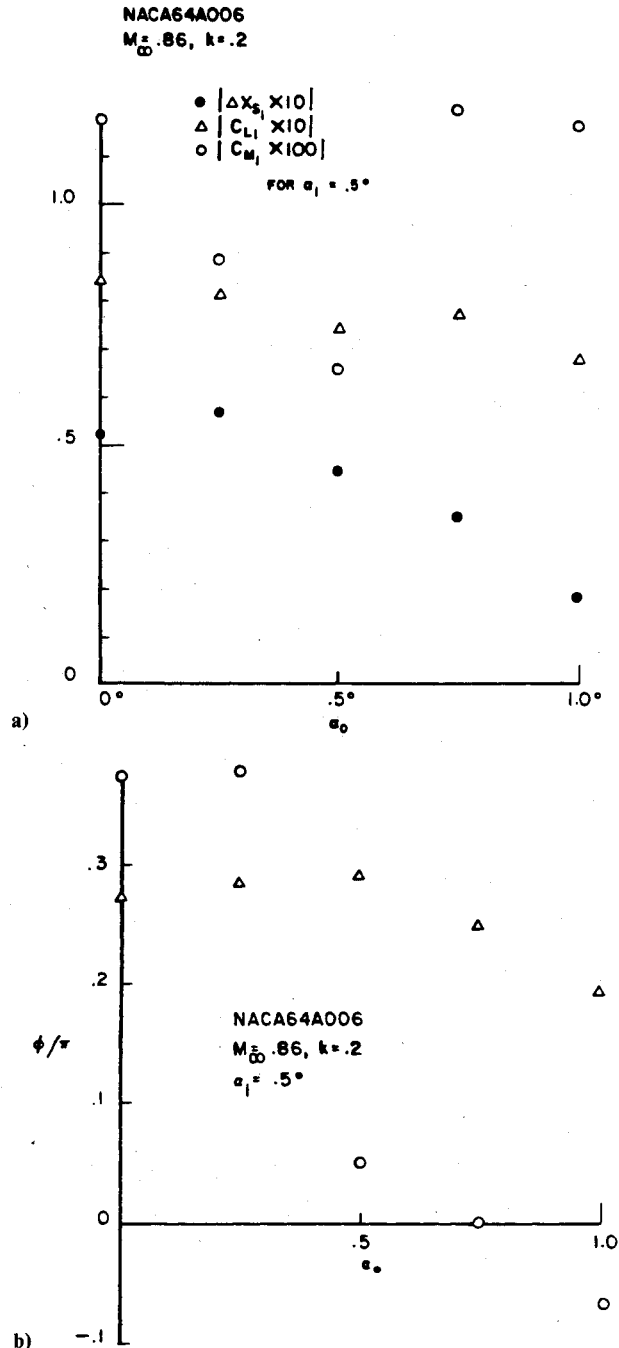


Fig. 10 Effect of steady-state angle of attack on dynamic forces and shock motions: a) amplitudes; b) phases.

where  $\bar{C}_p$  is a universal function of its arguments and

$$\beta \equiv (1 - M_\infty^2)^{1/2}, \nu \equiv k M_\infty^2 / \beta^2$$

$$K \equiv \frac{(\gamma + 1) M_\infty^2}{\beta^3}, s \equiv \frac{\beta^2 t U_\infty / c}{M_\infty^2}$$

$\tau$  = thickness ratio of airfoil

$\alpha$  = angle of attack

Equation (1) may be further specialized for the case  $\alpha \rightarrow 0$ , by expanding in a Taylor series, i.e.,

$$C_p = \frac{\tau}{\beta} \bar{C}_p(x/c; K) + \frac{\alpha}{\beta} \text{Re} \{ e^{i\nu s} \bar{C}_{p1}(x/c; K, \nu) \} \quad (2)$$

This is the similarity law for dynamic linearization in  $\alpha$ , i.e.,  $\alpha = \alpha_1$ . Zero mean angle of attack is assumed for simplicity,  $\alpha_0 = 0$ , although the result is readily extended. From Eq. (2), it is seen that similarity for the harmonic component requires only that  $K$  and  $\nu$  be the same for two different flows.

Finally, it is noted that since the shock is simply a discontinuity surface of  $\phi_x$ , it satisfies a similarity law expressed by

$$x_s = x_s(\beta y/c, s; K, \alpha/\tau, \nu) \quad (3)$$

For the limit,  $\alpha \rightarrow 0$ ,

$$x_s = x_{s0}(\beta y/c; K) + \alpha/\tau \operatorname{Re} \{ e^{i\nu x_{s1}}(\beta y/c; K, \nu) \} \quad (4)$$

The similarity law given by Eq. (1) was known to Miles.<sup>14</sup> Equations (2-4) are extensions of his results. See Ref. 13 for a derivation of these results.

Using the similarity rules, the results for the 64A006 airfoil may be used to obtain results for any other airfoil of the same family, in particular, the 64A010.

From Eq. (4) it may be inferred that the 5% shock motion criterion has the functional form (for a given family of airfoils)

$$\alpha/\tau = F(\nu, K) \quad (5)$$

It is interesting to note that Fung et al.<sup>10</sup> proposed a criterion for the validity of linearization of the form

$$\frac{\alpha}{\tau} / K \ll 0.1 \quad (6)$$

Equation (6) is clearly a special case of Eq. (5). Using Eq. (5), the data of Figs. 5, 6 (and 14, subsequently) may be reinterpreted in terms of similarity variables and thereby generalized.<sup>13</sup>

#### Flow at Zero Angle of Attack

It is instructive to consider first the flow over the airfoil at zero angle of attack. In particular, in Figs. 11a and 11b, the shock position and the shock strength (pressure jump across the shock) are shown as a function of freestream Mach number. These are determined approximately, but consistently, by using the following definitions:

1) The shock is located where the local Mach number is unity.

2) The pressure jump is from the pressure maximum just ahead of the shock to the pressure at the first subsonic mesh point behind the shock.

Note that the critical Mach number where the shock first appears is  $M_\infty^c = 0.824$ . The shock position at  $M_\infty = 0.84$  is  $x_{s0} = 0.48$  and it increases monotonically with  $M_\infty$ , reaching the trailing edge at  $M_\infty^c \approx 0.92$ . We shall call the latter the transcritical Mach number. As we shall see,  $M_\infty^c$  and  $M_\infty^c$  bound the essentially transonic Mach number range for this airfoil.

Also shown for reference are results from the nonconservative version of the full potential theory method of Bauer, Garabedian, and Korn.<sup>8</sup> Relative to LTRAN2, these results give a smaller pressure jump and a more forward shock location. As is well known, the latter two characteristics are, in part, attributable to the nonconservative solution algorithm.<sup>15</sup> See the subsequent discussion of Fig. 15.

#### Flow at Angle of Attack

In Fig. 12, the lift is presented vs angle of attack for steady flow,  $k=0$ . Note the behavior at  $M_\infty = 0.88, 0.9$  is nonlinear at much lower angles of attack than for  $M_\infty = 0.86, 0.92$ . For  $M_\infty < 0.86$  or  $> 0.92$  the behavior is linear to even larger angles of attack. Also note that the values of  $C_{L0}$  are much larger for  $M_\infty = 0.88, 0.90$ . Indeed, it is probable that at these

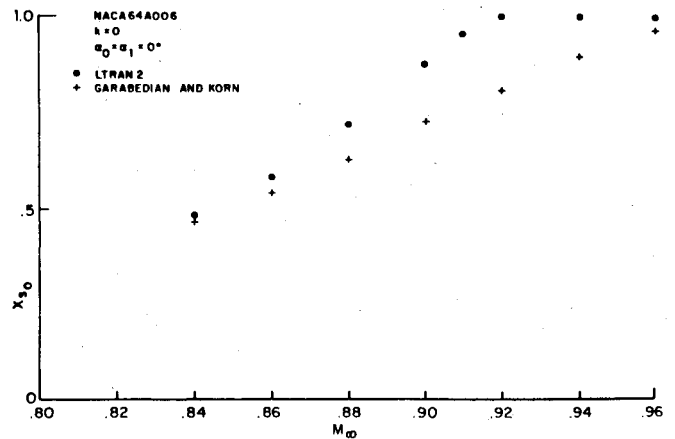


Fig. 11a Effect of freestream Mach number on shock position.

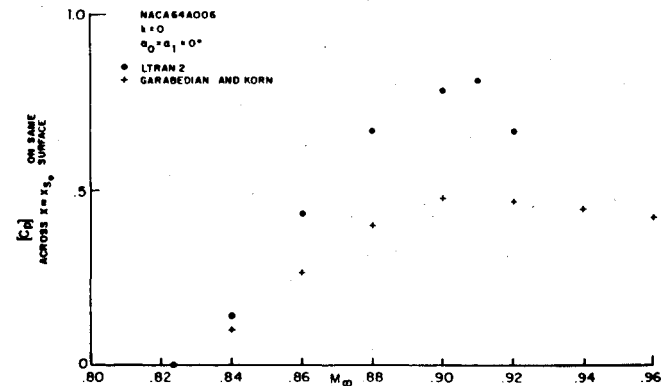


Fig. 11b Effect of freestream Mach number on pressure jump across shock.

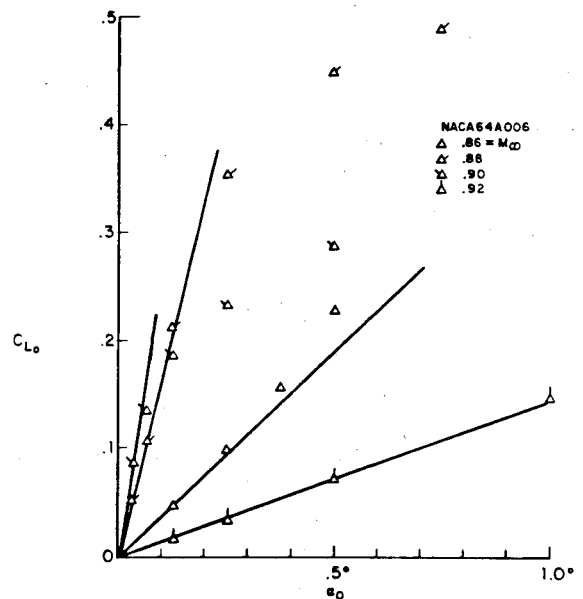


Fig. 12 Effect of freestream Mach number on lift vs angle of attack.

Mach numbers even the nonlinear transonic small disturbance theory is inadequate, except possibly at very small angles of attack.

In Figs. 13a and 13b, the corresponding differential pressure distributions are shown for  $M_\infty = 0.86$  and  $0.88$ . See Ref. 13 for  $M_\infty = 0.8, 0.84, 0.9$ , and  $0.92$ . The angle of attack was held constant at  $0.25^\circ$ . This is slightly outside the linear range of  $M_\infty = 0.88$  and well outside it for  $M_\infty = 0.9$ ; for other  $M$  the behavior is linear at  $\alpha_0 = 0.25^\circ$ .

To simplify the subsequent discussion, let us define the following two distinct pressure differences.

1)  $[C_p]$  = pressure jump across the shock at  $\alpha_0 = 0$ . This is the pressure difference from ahead of the shock to behind the shock on the same surface (upper or lower).

2)  $\Delta C_p$  = differential pressure. This is the pressure difference between the lower surface and the upper surface. It is zero for  $\alpha_0 = 0$  deg, of course, when the airfoil profile is symmetric.

Linear transonic theory<sup>4,5</sup> says the differential pressure,  $\Delta C_p$ , near the shock for any  $\alpha_0$  should be equal in magnitude to the pressure jump across the shock at  $\alpha_0 = 0$  deg,  $[C_p]$ . Note that linear transonic theory gives a reasonable value for the peak level of  $\Delta C_p$  in the vicinity of the shock even for  $M_\infty = 0.88$  and  $0.9$ . However, at the latter Mach numbers, the shock displacement appears too large. See Fig. 13 and Ref. 13.

Also shown in Fig. 13 is the differential pressure obtained using the supersonic Mach number just ahead of the shock and invoking classical supersonic theory via local linearization. For  $M_\infty = 0.92$  reasonable results are obtained ahead of the shock, which is at the trailing edge, and hence everywhere on the airfoil except near the leading edge.<sup>13</sup> For lower Mach numbers only a rough estimate is given by this approximation for  $\Delta C_p$  ahead of the shock. For  $M_\infty \geq 0.92$  local linearization is a useful tool, i.e., once the shock has reached the trailing edge. See subsequent discussion on this point also.

#### Linear/Nonlinear Behavior

Using results such as those shown in Fig. 12 and invoking the 5% shock displacement criterion, a linear/nonlinear boundary may be constructed. Of course, as the shock reaches

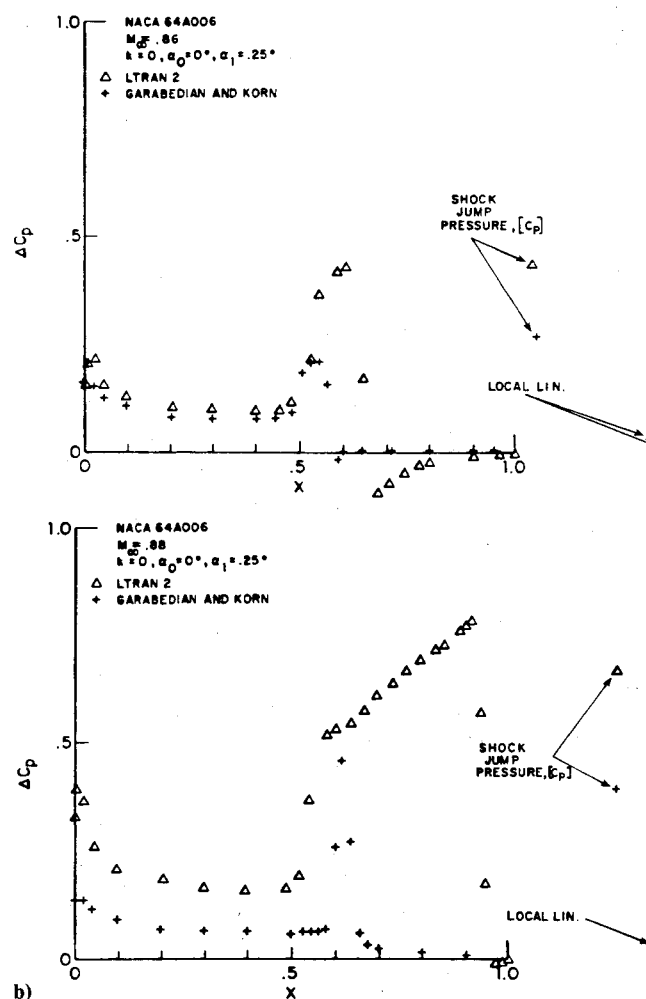


Fig. 13 Differential pressure distribution.

very near the trailing edge, the 5% criterion would need to be modified. Results are shown in Fig. 14 for  $k=0$  and  $0.2$ . Note that for steady flow ( $k=0$ ) the angle of attack must be very small when  $M_\infty = 0.88$  and  $0.9$  for linear behavior to occur. However, as we have seen before, the 5% shock displacement criterion is conservative. That is, lift and moment tend to remain linear in  $\alpha$  to higher  $\alpha$  than this criterion would suggest. Nevertheless, the trend should not change using any other reasonable criterion. By contrast, for  $k=0.2$  the linear region is much enlarged. For  $M_\infty < M_\infty^c$  or  $M_\infty > M_\infty^c$  the linear region is for all practical purposes unbounded. In practice, in this region other physical effects, e.g., viscosity, are likely to come into play before inviscid, small disturbance, transonic theory nonlinearities become important. Figure 14 is a principal result of the present work.

#### Aerodynamic Transfer Functions

In the linear region it is of interest to display aerodynamic transfer functions vs Mach number. Perhaps the most familiar of these is lift curve slope,  $C_{L_\alpha}/\alpha_1$ . Its amplitude is shown in Fig. 15a from LTRAN2 for  $k=0$ . Also shown are results from full potential theory, classical subsonic theory, and local linearization. The latter is shown for  $M_\infty > M_\infty^c$ , i.e., the shock is at the trailing edge. It uses the local trailing edge supersonic Mach number in classical (supersonic) theory. One concludes that for  $M_\infty < M_\infty^c$ , classical theory gives reasonable results, and for  $M_\infty > M_\infty^c$  local linearization gives reasonable results. For  $M_\infty^c < M_\infty < M_\infty^{tc}$ , LTRAN2 gives markedly different results although it likely fails for  $M_\infty = 0.88, 0.90$ . Note the difference between transonic small disturbance theory (LTRAN2) which falls well off scale at  $M_\infty = 0.88$  and  $0.9$  and full potential theory (BGK).

It should be noted that the full potential results shown in Fig. 15a were obtained using a nonconservative finite difference scheme. Full potential results obtained using a quasiconservative finite difference scheme (for technical reasons results were only obtained for  $M_\infty \leq 0.87$ ) are essentially identical to those of transonic small disturbance theory using a conservative finite difference scheme (LTRAN2). Hence, the difference shown in Fig. 15a should be attributed to the distinction between conservative and non-conservative finite differences and not to the distinction between small disturbance and full potential theory. To the extent that the nonconservative finite difference method may be said to have some form of numerical (as opposed to

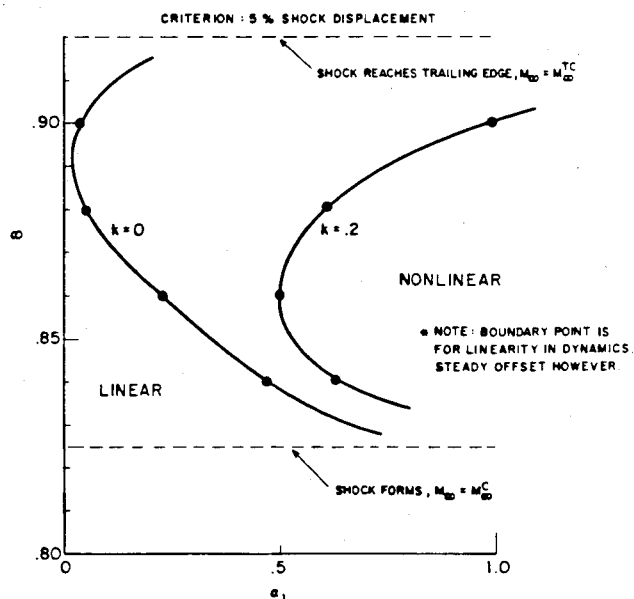


Fig. 14 Effect of frequency on boundary for linear/nonlinear behavior.

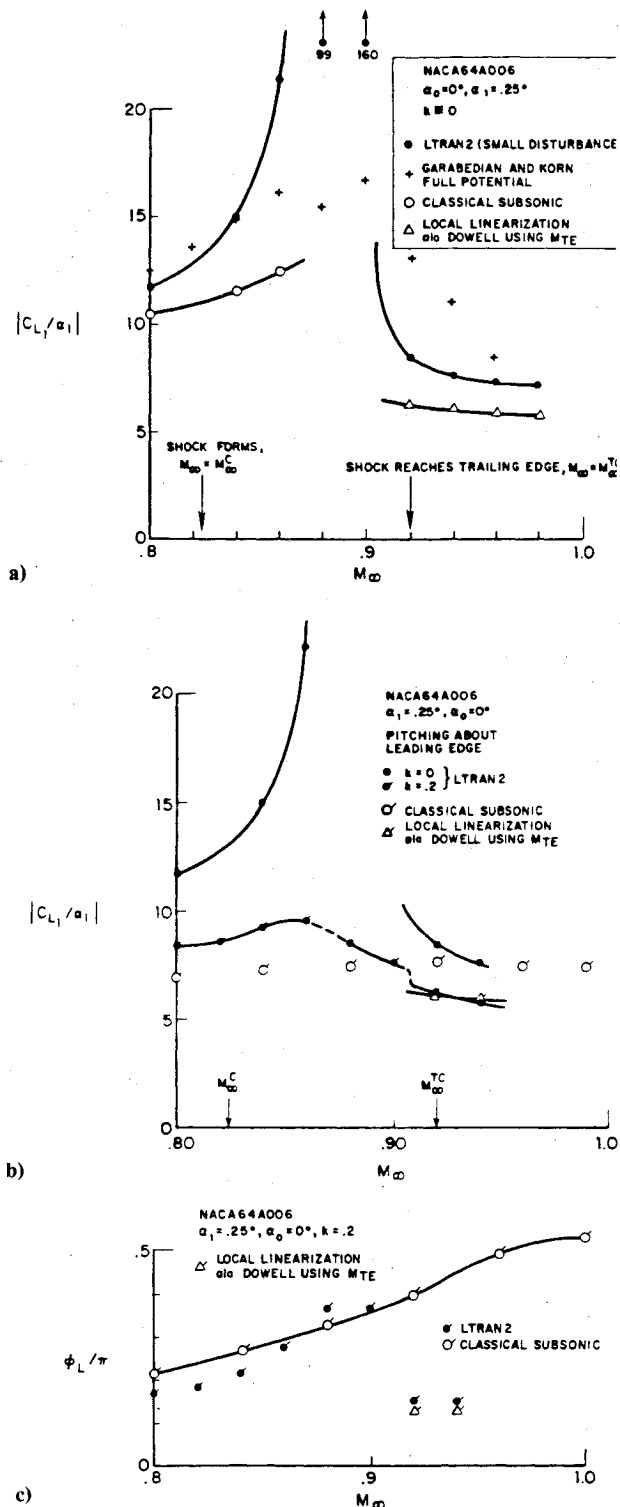


Fig. 15 Effect of freestream Mach number on a) and b) lift curve slope; c) phase of lift relative to pitch.

physical) viscosity, the differences may be attributed to the qualitative distinction between inviscid and viscous flow.

In Fig. 15b results are shown for  $k=0.2$ . For reference, the LTRAN2 results for  $k=0$  are also shown. Again it is seen that the classical subsonic theory and local linearization theory give reasonable results (better than for  $k=0$ ) for  $M_\infty < M_\infty^C$  and  $M_\infty > M_\infty^{TC}$ , respectively. Moreover, LTRAN2 appears to give reasonable results over the entire Mach number range, although there is no better theory to validate it. Note that from  $M_\infty = 0.9$  to  $0.92$  there is a somewhat abrupt change.

In Fig. 15c the phase of the lift curve slope is shown. Perhaps surprisingly, classical subsonic theory and local

linearization do rather well. Note the abrupt change in phase as the shock reaches the trailing edge. Recall the corresponding variation of lift amplitudes in Fig. 15b.

Similar results (not shown) were obtained for pitching moment.<sup>13</sup>

### Conclusions

For  $M_\infty < M_\infty^C$ , where no shock exists, the aerodynamic forces are linear over a substantial range of angle of attack. This is also true for  $M_\infty > M_\infty^{TC}$ , i.e., where the shock has moved to the trailing edge. For  $M_\infty^C < M_\infty < M_\infty^{TC}$  a boundary of linear/nonlinear behavior may be constructed which shows the angle of attack must be quite small for linear behavior to occur for *steady* flow. However the region of linear behavior increases substantially for *unsteady* flow.

In the range  $M_\infty^C < M_\infty < M_\infty^{TC}$  transonic small disturbance theory (LTRAN2) and full potential theory appear to fail for *steady* flow for some narrow band of  $M_\infty$  where they substantially overestimate the shock displacement and, hence, the aerodynamic forces. This is tentatively attributed to the absence of viscosity in the theories.

Classical subsonic theory and local linearization are useful approximate tools for unsteady flow provided their limitations are recognized.

Aerodynamic transfer functions are expected to retain their utility even when nonlinear dynamic effects are important. This is for several reasons, including:

- 1) Nonlinear effects diminish with increasing frequency.
- 2) At high frequencies, classical linear theory is expected to be reasonably accurate and indeed most inviscid theories will approach classical theory as the frequency becomes large.<sup>4,5</sup>
- 3) The preceding suggests that several theories may be used to provide a composite aerodynamic representation in the frequency domain. For example, one might use BGK for  $k=0$ , LTRAN2 for  $k=0.05-0.2$ , Williams for  $k=0.2-1.0$ , and classical theory (which Williams' theory smoothly approaches) for  $k>1.0$ .

A similarity law for low frequency transonic small disturbance theory is available which reduces the number of aerodynamic computations required and generalizes results for one airfoil to an entire family.

Although two-dimensional flows have been treated here, the general concepts and approach should be useful for three-dimensional flows. In particular, one expects the effect of three-dimensionality to increase the region of linear behavior for transonic flows. For example, the accuracies of transonic small disturbance theory, local linearization, and classical theory should be enhanced by three-dimensional effects.

No transonic method of aerodynamic analysis can be expected to give useful information to the aeroelastician unless the mean steady flow it predicts and uses is accurate. Hence, it is highly desirable to be able to input directly the best steady flow information which is available including that from experiment. The latter would include implicitly viscosity effects on the mean steady flow; in particular it would place the mean shock in the correct position.

The reader may wish to consult the lucid survey article by Tijdeman and Seebass<sup>12</sup> which provides a context in which to evaluate the present results and conclusions. Also Nixon and colleagues have discussed extensively how the transonic, linear theory may be used in aeroelastic analyses. For example, see Refs. 16 and 17.

### Acknowledgment

This work was done while the first author was resident at NASA Langley Research Center.

### References

- 1 Ballhaus, W.F. and Goorjian, P.M., "Implicit Finite Difference Computations of Unsteady Transonic Flows about Airfoils," *AIAA Journal*, Vol. 15, Dec. 1977, pp. 1728-1735.



<sup>2</sup>Ballhaus, W.F. and Goorjian, P.M., "Efficient Solution of Unsteady Transonic Flows about Airfoils," Paper 14, *AGARD Conference Proceedings* No. 226, Unsteady Airload in Separated and Transonic Flows, 1978.

<sup>3</sup>Davis, S.S. and Malcolm, G., "Experiment in Unsteady Transonic Flows," *Proceedings of the AIAA/ASME/ASCE 20th Structures, Structural Dynamics and Materials Conference*, St. Louis, Mo., April 1979.

<sup>4</sup>Williams, M.H., "The Linearization of Transonic Flows Containing Shocks," *AIAA Journal*, Vol. 17, April 1979, pp. 394-397.

<sup>5</sup>Williams, M.H., "Unsteady Thin Airfoil Theory for Transonic Flows with Embedded Shocks," *AIAA Journal*, Vol. 18, June 1980, pp. 615-624; also see "Unsteady Airloads in Supercritical Transonic Flows," *Proceedings of the AIAA/ASME/ASCE 20th Structures, Structural Dynamics and Materials Conference*, St. Louis, Mo., April 1979.

<sup>6</sup>Yang, T.Y., Stritz, A.G., and Guruswamy, P., "Flutter Analysis of Two-Dimensional and Two-Degree-of-Freedom Airfoils in Small-Disturbance Unsteady Transonic Flow," AFFDL-TR-78-202, Dec. 1978.

<sup>7</sup>Magnus, R.J. and Yoshihara, H., "Calculations of Transonic Flow Over an Oscillating Airfoil," AIAA Paper 75-98, Jan. 1975.

<sup>8</sup>Bauer, F., Garabedian, P., and Korn, D., "Supercritical Wing Sections," *Lecture Notes in Economics and Mathematical Systems*, Vol. 66, Springer-Verlag, 1972.

<sup>9</sup>Tijdeman, H. and Schippers, P., "Results of Pressure Measurements on an Airfoil with Oscillating Flow in Two-

Dimensional High Subsonic and Transonic Flow," National Aerospace Laboratory, the Netherlands, NLR TR-730780, July 1973.

<sup>10</sup>Fung, K.Y., Yu, N.J., and Seebass, R., "Small Unsteady Perturbations in Transonic Flows," *AIAA Journal*, Vol. 16, Aug. 1978, pp. 815-822.

<sup>11</sup>Tijdeman, H., "Investigations of the Transonic Flow Around Oscillating Airfoils," Ph.D. Thesis, Delft University, Dec. 1977.

<sup>12</sup>Tijdeman, H. and Seebass, R., "Transonic Flow Past Oscillating Airfoils," *Annual Review of Fluid Mechanics*, Vol. 12, 1980, pp. 181-222.

<sup>13</sup>Dowell, E.H., Bland, S.R., and Williams, M.H., "Linear/Nonlinear Behavior in Unsteady Transonic Aerodynamics," Princeton University, MAE Rept. 1520, May 1981.

<sup>14</sup>Miles, J.W., *The Potential Theory of Unsteady Supersonic Flow*, Cambridge University Press, 1959, pp. 4-13.

<sup>15</sup>Jameson, A., "Transonic Potential Flow Calculation Using Conservation Form," *Proceedings of the AIAA Second Computational Fluid Dynamics Conference*, Hartford, Conn., June 1975, pp. 148-161.

<sup>16</sup>Nixon, D. and Kerlick, G.D., "Calculation of Unsteady Transonic Pressure Distributions by Indicial Methods," Nielsen Engineering and Research Paper 117, 1980.

<sup>17</sup>Nixon, D., "On the Derivation of Universal Indicial Functions," AIAA Paper 81-0328, Jan. 1981.

## *From the AIAA Progress in Astronautics and Aeronautics Series . . .*

### **AERO-OPTICAL PHENOMENA—v. 80**

*Edited by Keith G. Gilbert and Leonard J. Otten, Air Force Weapons Laboratory*

This volume is devoted to a systematic examination of the scientific and practical problems that can arise in adapting the new technology of laser beam transmission within the atmosphere to such uses as laser radar, laser beam communications, laser weaponry, and the developing fields of meteorological probing and laser energy transmission, among others. The articles in this book were prepared by specialists in universities, industry, and government laboratories, both military and civilian, and represent an up-to-date survey of the field.

The physical problems encountered in such seemingly straightforward applications of laser beam transmission have turned out to be unusually complex. A high intensity radiation beam traversing the atmosphere causes heat-up and breakdown of the air, changing its optical properties along the path, so that the process becomes a nonsteady interactive one. Should the path of the beam include atmospheric turbulence, the resulting nonsteady degradation obviously would affect its reception adversely. An airborne laser system unavoidably requires the beam to traverse a boundary layer or a wake, with complex consequences. These and other effects are examined theoretically and experimentally in this volume.

In each case, whereas the phenomenon of beam degradation constitutes a difficulty for the engineer, it presents the scientist with a novel experimental opportunity for meteorological or physical research and thus becomes a fruitful nuisance!

412 pp., 6×9, illus., \$30.00 Mem., \$45.00 List

TO ORDER WRITE: Publications Dept., AIAA, 555 West 57th Street, New York, N.Y. 10019